International Journal of Pharmaceutics 364 (2008) 45–53

Contents lists available at ScienceDirect

International Journal of Pharmaceutics

journal homepage: www.elsevier.com/locate/ijpharm

Kinetics of solvent extraction/evaporation process for PLGA microparticle fabrication

Hajime Katou[a,*], Anne Julia Wandrey[b], Bruno Gander[b]

[a] Tsuchiura Research Laboratory, Hitachi Plant Technologies Ltd., 603 Kandatsu, Tsuchiura, Ibaraki 300-0013, Japan
[b] Institute of Pharmaceutical Science, ETH Zurich 8093, Switzerland

ARTICLE INFO

Article history:
Received 6 July 2008
Accepted 4 August 2008
Available online 22 August 2008

Keywords:
Solvent extraction
Solvent diffusion
Mathematical model
PLGA
Microparticle fabrication

ABSTRACT

Organic solvent extraction/evaporation from an o/w-dispersion has been widely used for the fabrication of PLGA microparticles. The purpose of this work was to elucidate the kinetics of the solvent extraction/evaporation process. A mathematical diffusion model was developed and applied to predict the duration of the solvent extraction. As the diffusion coefficient, D_p, plays a major role in the modeled process, a new and experimentally simple method for estimating D_p was developed. Both the experimental method and the mathematical model were validated through PLGA microparticle fabrication experiments. For microparticles of mode diameters of 2 and 20 μm, the solvent was extracted in approximately 10 s. Sufficient hardening of the microparticles required, however, the evaporation of solvent from the extraction phase. Residual solvent in extraction phase exerted a strong effect on the morphology of the final product as demonstrated by scanning electron microscopy. Only if most solvent was removed from the aqueous extraction phase, a powdery product of individual microparticles was obtained. At residual organic solvent concentration of above 0.2% in the extraction phase, the microparticles strongly aggregated during collection on a membrane filter and final drying. The presented methods may be useful for better controlling microparticle fabrication processes by solvent extraction/evaporation.

1. Introduction

Biodegradable poly(lactide-co-glycolide) (PLGA) or poly(lactic acid) (PLA) microparticles for controlled drug delivery are frequently fabricated by organic solvent extraction from o/w- or w/o/w-emulsions. The performance and robustness of the fabrication processes have successfully been optimized by well-controlled emulsification techniques (Freitas et al., 2004, 2005; Berkland et al., 2001) and the composition of the o- and w-phases (solvents and other additives) (Zhang and Zhu, 2004; Graves et al., 2005; Chen et al., 2004). Various studies have also elucidated the most important physical chemical parameters controlling the solvent extraction process (Wang and Schwendeman, 1999; Li et al., 1995a,b; Maa and Hsu, 1996). Such parameters are critical for modeling the process steps, which in turn may be of general significance for, e.g. (i) fabrication of micro- and nanoparticles from different materials, (ii) scaling the process to pilot or production level, and (iii) introduction of automation technologies.

A review of the literature has revealed that the modalities and duration of solvent extraction and solvent evaporation from the process system still much depends on empirical know-how. To predict the duration of the solvent extraction, the diffusion coefficient of the solvent in polymer solution is an important parameter. To determine the solvent diffusion coefficient, experimentally developed equations like the Wilke–Chang equation (Wang and Schwendeman, 1999) and others (Li et al., 1995a) have been used. These equations require empirical parameters and approximations, which are strongly material dependent.

In addition to the solvent diffusibility in the polymer phase, the amount of solvent in the extraction phase is also a critical parameter. The solvent extracted from the o/w- or w/o/w-emulsions must eventually be removed from the extraction phase to obtain solid particles. We noticed that there is very little data and discussion on the relationship between the amount of residual solvent in the extraction phase and the quality of the final particulate product (micro- or nanoparticles).

In this work, we aimed at elucidating the kinetics of solvent extraction and evaporation from an o/w-dispersion. In particular, we developed a mathematical model describing the kinetics of solvent transport from the o-phase into the surrounding w-phase (extraction phase). Moreover, we investigated the influence of the amount of residual solvent in the extraction phase on the

* Corresponding author. Tel.: +81 29 832 9085.
E-mail addresses: hajime.kato.sx@hitachi-pt.com, hfkato@jcom.home.ne.jp (H. Katou).

0378-5173/$ – see front matter © 2008 Elsevier B.V. All rights reserved.
doi:10.1016/j.ijpharm.2008.08.015

morphology of the final product. We expect that the model and derived knowledge will assist in future process design optimization (automation, up-scaling) and provide information on the conditions needed (fluid dynamics, process time) to obtain solid particles that can readily be separated from the processing liquid.

2. Model development

Fig. 1 illustrates the basic steps of commonly used solvent extraction/evaporation processes for PLGA micro- and nanoparticle fabrication. In Step 1, a solution of polymer in an organic solvent is emulsified into an aqueous extraction phase generating the initial stage of microparticle shaping. In Step 2, the organic solvent of the polymer phase droplets is extracted into the surrounding aqueous extraction phase; this process is governed by solvent diffusion along its concentration gradient between the two phases. In this step, the droplets transform into semi-solid or solid particles, which still contain residual organic solvent and water. In Step 3, the extracted organic solvent is evaporated to a sufficient extent from the aqueous extraction phase. At completion of this step, the slurry consists of polymeric particles and aqueous extraction phase with ideally minimal residual organic solvent. Commonly, the solid particles are separated from the slurry by collection on a membrane filter or by centrifugation (step 4) and dried (step 5).

In a typical particle fabrication process, Steps 2 and 3 occur simultaneously. Past endeavors to model the solvent extraction/evaporation process have indeed considered the simultaneous occurrence of Steps 2 and 3 (Wang and Schwendeman, 1999; Li et al., 1995a,b; Maa and Hsu, 1996). Nonetheless, the solvent extraction from the polymer phase droplets and the solvent evaporation from the extraction phase are different processes, which deserve individual consideration for better understanding their importance.

Of particular practical importance is the duration of Step 2, i.e., the time needed for solvent extraction. To elucidate the kinetics of solvent extraction, two mathematical models were developed. The first model was derived from a diffusion equation to calculate the solvent extraction time from polymer phase droplets (Step 2). The second model was developed to obtain valid solvent diffusion coefficient values in the polymer phase. The model was derived from experimental data on solvent evaporation from a polymer solution, as described in Section 3.3.

2.1. Model for solvent extraction from polymer phase droplets into surrounding aqueous phase

For the solvent extraction step, a diffusion equation for a single polymer solution droplet surrounded by aqueous extraction phase was defined. Assuming central symmetry, the solvent diffusion is expressed as

$$\frac{\partial c_d}{\partial t} = \frac{D_p}{r^2}\frac{\partial}{\partial r}\left(r^2\frac{\partial c_d}{\partial r}\right) \quad (1)$$

where c_d stands for solvent concentration, t for time, r for radial position, and D_p for the solvent diffusion coefficient in the polymer solution. Although the real diffusibility depends on the solvent concentration in the polymer phase, the diffusion coefficient was assumed to be constant. At the center of the droplet ($r=0$), the boundary condition can be defined as

$$\left.\frac{\partial c_d}{\partial r}\right|_{r=0} = 0 \quad \text{at } r = 0 \quad (2)$$

At the droplet surface ($r=R$), where the solvent molecules pass from the inner to the outer side of the droplet, the boundary condition is defined as

$$D_p\left.\frac{\partial c_d}{\partial r}\right|_{r=R-0} = D_E\left.\frac{\partial c_d}{\partial r}\right|_{r=R+0} \quad \text{at } r = R \quad (3)$$

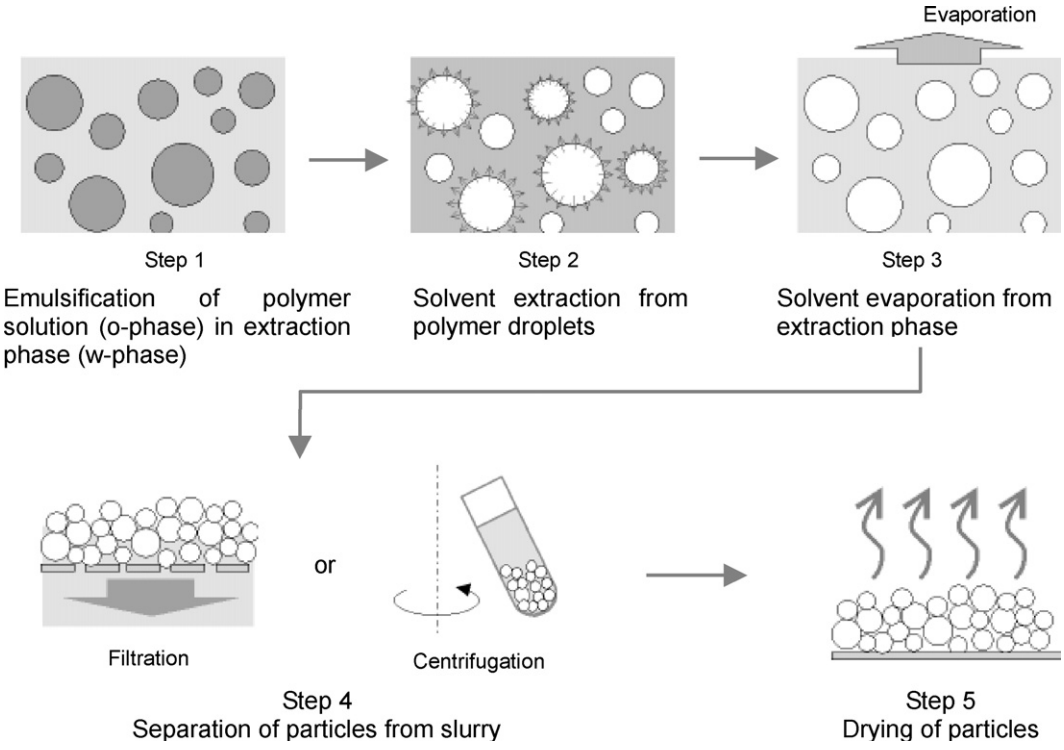

Fig. 1. Schematic illustration of the PLGA microparticle fabrication process by organic solvent extraction/evaporation from an o/w-emulsion.

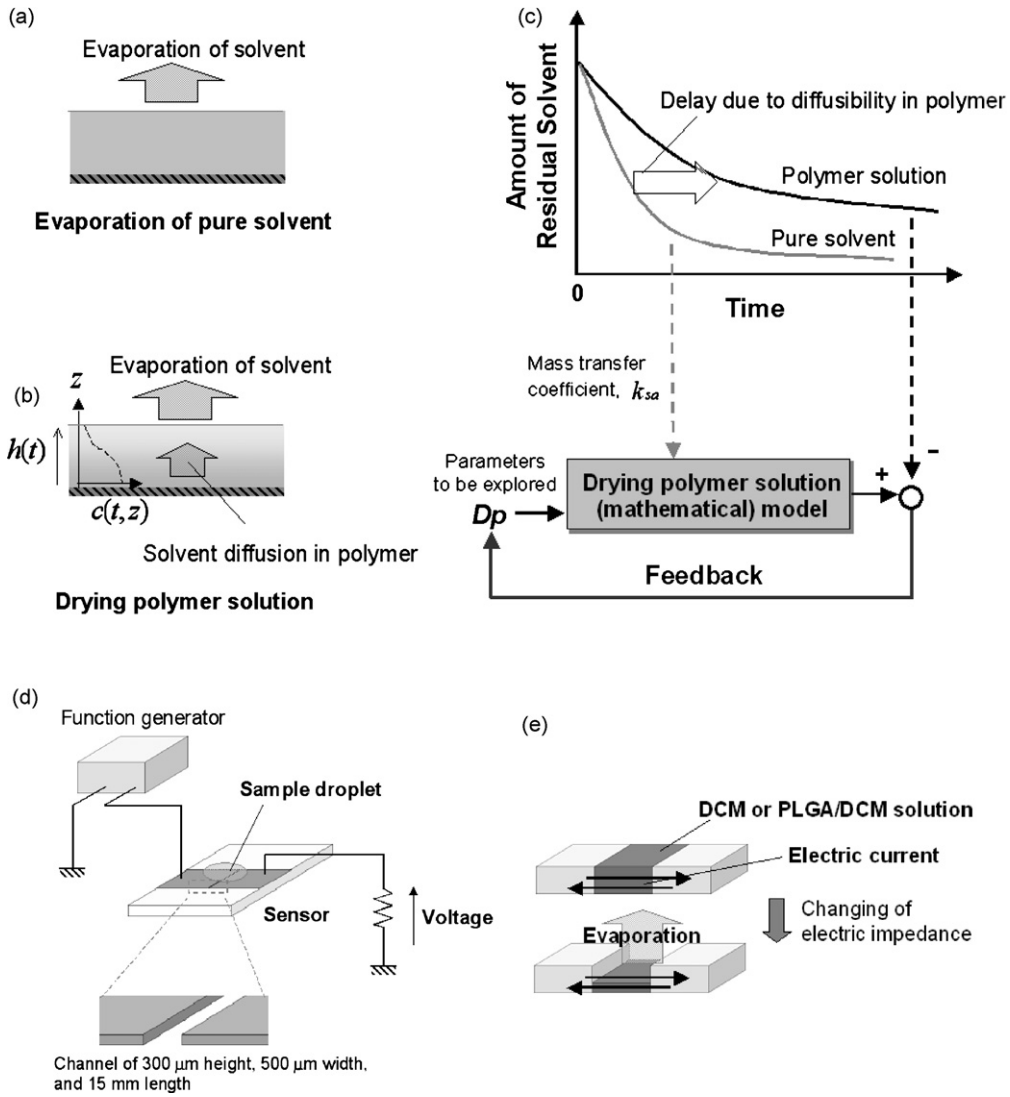

Fig. 2. Prediction of DCM diffusibility: (a) in pure DCM (evaporation of DCM); (b) in PLGA/DCM solution (evaporation and diffusion of DCM in polymer (PLGA)); (c) algorithm for optimizing the prediction of diffusion coefficient of DCM in polymers from experiments (a) and (b); (d) schematic illustration of the developed sensor system to measure the evaporation of DCM from pure solvent and PLGA/DCM solution; (e) operation principle of the sensor.

where D_E is the solvent diffusion coefficient in the aqueous extraction phase and R is the radius of the droplet.

2.2. Model for determining solvent diffusion coefficient during solvent evaporation from a polymer solution

The model developed for determining the solvent diffusion coefficient during solvent evaporation from a polymer solution was based on a polymer solution with constant surface area S, from where the solvent is evaporated in a one direction leading to the formation of a film. Henceforth, the experimental system will be referred to as polymer solution/film. The experimental basis for the model development is illustrated in Fig. 2(b). The solvent mass balance in the polymer solution can be expressed by

$$\frac{\partial c_{df}}{\partial t} = \frac{\partial}{\partial z}\left(D_p \frac{\partial c_{df}}{\partial z}\right) \tag{4}$$

where c_{df} is the solvent concentration in the polymer solution, t the time, and z is the vertical position in the solution. As solvent evaporation is restricted to one direction, the boundary condition at $z = 0$ is defined as

$$\frac{\partial c_{df}}{\partial z} = 0 \quad \text{at } z = 0 \tag{5}$$

The solvent flux at the surface of the polymer solution/film results from the interfacial mass balance, which consists of diffusion and evaporation of the solvent. The mass balance is expressed as

$$-D_p \frac{\partial c_{df}}{\partial z} + c_{df} \frac{\partial h}{\partial t} = -n_d \quad \text{at } z = h(t) \tag{6}$$

where $h(t)$ is the thickness of the polymer solution/film at time t, i.e. the position of the solution/film surface, and n_d is the flux through the solution/film surface, i.e. the evaporation rate. During solvent evaporation, the thickness of the solution/film layer decreases. Introducing a term for the specific volume of the polymer solution/film $\nu(c_{df})$, which is primarily a function of the solvent concentration or mass fraction, the decreasing volume of the solution/film can be obtained, and the thickness is expressed as

$$h = \frac{1}{S}\int_M \nu(c_{df})\, dm \tag{7}$$

where S is the constant evaporation area of the solution/film, dm an infinitesimal mass, and M is the total mass of the solution/film (sum of polymer and solvent components). During evaporation, the mass of the solvent decreases according to

$$\frac{\partial M}{\partial t} = -Sn_{\mathrm{d}} \tag{8}$$

Integration of Eq. (8) provides the initial total mass of the polymer solution/film.

The solvent flux through the polymer solution/film surface, i.e. the evaporation rate, is the driving force determining the kinetics of the drying process. Several studies have already examined and described the solvent evaporation rates from polymer solutions (Birdi et al., 1989; Rowan et al., 1995; Price and Cairncross, 1999; Erbil and Dogan, 2000; Babin and Holyst, 2005; Hopkins and Reid, 2005; Fang et al., 2005; Li et al., 2006). Price and Cairncross (1999), Erbil and Dogan (2000) and Fang et al. (2005) have expressed the solvent evaporation rate as a function of solvent vapor pressure and mass transfer coefficient. In the present study, we quantified the solvent flux by

$$n_{\mathrm{d}} = k_{\mathrm{sa}}\alpha P_{\mathrm{evp}}^{\mathrm{slv}} \tag{9}$$

where k_{sa} is the mass transfer coefficient, α the activity of the solvent in the solution, and $P_{\mathrm{evp}}^{\mathrm{slv}}$ is the vapor pressure of the pure solvent. The mass transfer coefficient was experimentally determined (see Section 3.3). The solvent activity is a function of the volume fraction of the solute (polymer) in the solution and, therefore, it depends on the solvent concentration at surface (at $z = h(t)$). The relationship between the activity and the volume fraction or the concentration was determined according to the Flory–Huggins theory (Flory, 1978). The necessary molecular interaction parameter between solvent and polymer was deduced from the literature (Eser and Tihminlioglu, 2006).

In this model, the concentration c_{df}, the concentration dependent local specific volume $\nu(c_{\mathrm{df}})$, and the thickness $h(t)$ are variables to express the physical state of the polymer solution/film. Given the initial conditions and materials properties (i.e., solution/film dimensions, initial solute concentration, solvent diffusion coefficient in the film, and the relationship between specific solvent volume and its concentration), the total mass of the polymer solution/film and the residual mass of solvent were determined from Eqs. (8) and (9). The mass transfer coefficient in Eq. (9) depends on the solvent. In the present study, the coefficient was experimentally obtained by using the method described in Section 3.3.

3. Methods

3.1. Materials

The biodegradable polymer used was an end-group uncapped 35 kDa poly(lactide-co-glycolide) 50:50 (PLGA 50:50) from Boehringer-Ingelheim, Ingelheim, Germany (Resomer RG503H). Solutions of 7.5% (w/w) PLGA in dichloromethane (DCM) were used unless described otherwise. Double distilled water was used as extraction phase.

3.2. Specific volume of polymer solution

The specific volume of the polymer solution/film $\nu(c_{\mathrm{df}})$ (Eq. (7)), which is primarily a function of the solvent concentration, was experimentally determined by monitoring the shrinking of PLGA solution/film. The measurement was made with solutions of 5, 10, 20 and 50% (w/w) PLGA in DCM. Weight and volume of each solution were first measured accurately (pycnometer) to obtain the mass fractions of the components and the specific volumes of the polymer solutions. For determining the volumes at lower DCM concentration, the PLGA solutions were kept under ambient condition to let the solvent evaporate in dishes of well-defined dimensions. In this process, the PLGA solution shrank and turned into a gel. The thickness and weight of the gels were measured with a micrometer and a microbalance respectively, and the mass fraction and specific volume of the gel (at low DCM concentrations) were determined.

3.3. Prediction of solvent diffusibility in PLGA

The experimental setup and related data analysis model to predict the diffusibility of solvent in PLGA/DCM solution is illustrated in Fig. 2. In this method, the kinetics of solvent evaporation from PLGA/DCM solution and pure solvent (DCM) was measured as outlined below. The solvent evaporation rate from the polymer solution was substantially lower than from the pure solvent, which is due to the lower solvent activity and increasing viscosity of the polymer solution. From this difference in solvent evaporation rates under otherwise identical experimental conditions, the DCM diffusibility in PLGA/DCM solution was determined. Although the actual diffusibility depends on the solvent concentration, we assumed, for simplicity, a constant diffusion coefficient in the sol and gel states of the sample (Li et al., 1995a).

With pure DCM (Fig. 2(a)), mass decrease was solely caused by evaporation so that Eq. (9) with $\alpha = 1$ (i.e., constant maximal activity) could be applied. According to Eq. (8), the evaporation rate of pure DCM corresponds to $\partial M/\partial t = -Sk_{\mathrm{sa}}P_{\mathrm{evp}}^{\mathrm{slp}}$. From the time-derivative of the measured mass loss profile, the mass transfer coefficient of DCM, k_{sa}, was determined.

For the PLGA/DCM solution, the solvent evaporation was calculated by Eqs. (4)–(9) using the previously determined solvent mass transfer coefficient k_{sa}. The calculations were reiterated using varying diffusion coefficients to minimize the difference between the measured and calculated profiles and to obtain the diffusion coefficient of the system.

Solvent evaporation from pure DCM or PLGA/DCM solution was quantified by electric conductivity measurements (Fig. 2(d) and (e)). The measuring system consisted of a function generator (33250A, Agilent Technologies, CA, USA), a custom-made electrical sensor, and a 22 kΩ resistance unit (Fig. 2(d)). The sensor consisted of two electrodes glued on a glass plate and separated by a small channel of 300 μm height, 500 μm width, and 15 mm length (Fig. 2(d), bottom part with zoomed-in view). When filled with an electrically conductive material, the sensor unit measures a change of electric current. The conductance depends on the properties and the amount of the material (Fig. 2(e)). Therefore, by supplying constant voltage amplitude from the function generator, the amount of the material remaining in the channel during solvent evaporation could be detected by the voltage generated on the resistance unit. Although the electric conductivity of the organic phase was very low, preliminary testing revealed that alternate current of 1.1 MHz, 5 V (peak to peak) is optimal in terms of signal-to-noise (S/N) ratio for this measurement. The detected voltage signal was also an alternate current so that the magnitude of the signal had to be transferred to the effective voltage with a rectifier circuit. This allowed us to monitor continuously the decreasing amount of sample on a computer (CF-R1, Panasonic, Osaka, Japan) equipped with analog I/O card device (ADA16-8/2(CB)L, CONTEC, Osaka, Japan).

3.4. Fabrication of PLGA microparticles

PLGA/DCM solution (o-phase) was emulsified in pure water (w-phase) (Fig. 1, Step 1) by a micromixer (Micro Process Server™, MPS-α100, Hitachi Plant Technologies, Tokyo, Japan), which has

recently been developed. This mixer is a continuous flow-through type mixer in which liquid phases (e.g., o-phase and w-phase) are forced through a microchannel to generate high-shear forces for mixing or emulsification. The ratio of o/w (v/v) was set at 1/10, and total flow rate of materials was varied from 22 to 110 ml/min to vary droplet sizes. Although the mixer can process liquids continuously, the batch volume of o/w-dispersion used in this study was 27.5 ml (2.5 ml of o-phase and 25 ml of w-phase).

As mentioned above, solvent extraction into the extraction phase (Fig. 1, Step 2) and solvent evaporation from the extraction phase (Fig. 1, Step 3) were separately operated in this work according to the following protocol. For solvent extraction, the dispersion was discharged from the mixer into a measuring cylinder pre-filled with 500 ml extraction phase (pure water) and stirred gently to extract DCM from the o/w-dispersion (Fig. 1, Step 2). Here, the ratio (v/v) of DCM/water was more than 1: 250 to ascertain sufficient water phase capacity for dissolving all DCM (solubility of DCM in water is approx. 1.0%, v/v). To minimize solvent evaporation at this stage, the liquid/air interface was kept small by using a cylindrical vessel (diameter of 50 mm; liquid height of 255 mm), the mixture was stirred only gently, and the cylinder sealed tightly to retain the solvent in the o/w-dispersion. The time allowed for this solvent extraction step was varied between 0 and 15 min.

The second process, i.e., the solvent evaporation from the extraction phase (Fig. 1, Step 3), was performed by transferring the o/w-dispersion into a glass dish of 200 mm diameter and vigorous stirring to provide a large liquid/air interface and promote the DCM evaporation from the extraction phase. The time allowed for this solvent evaporation step was varied between 0 and 45 min. At the end of this process, the PLGA particles were solidified and ready for collection on a 0.45 μm pore-size membrane filter (cellulose acetate, OE67, Whatman, Dassel, Germany) (Fig. 1, Step 4); the collected microparticles were finally dried at 20 mbar and room temperature for 24 h (Fig. 1, Step 5).

3.5. Rate of solvent evaporation from extraction phase

The rate of solvent evaporation from the extraction phase (Fig. 1, Step 3) was measured by monitoring over time the total weight of the o/w-dispersion, according to the PLGA microparticle fabrication protocol. As total weight decrease was due to the evaporation of both DCM and water (extraction phase), the evaporation rate from 500 ml of pure water was measured as a control and subtracted from total evaporation; the amount of water evaporating in the azeotrope mixture with DCM was neglected as it amounts only to 1% (w/w) of the azeotrope.

3.6. Particle size distribution

Particle size distributions were measured by laser light scattering (Mastersizer X, Malvern, Worcestershire, UK, equipped with a 100-mm lens) using a Fraunhofer diffraction model. For convenience, the microparticles were analyzed for size before their final drying.

3.7. Morphology of microparticles (scanning electron microscopy)

Samples of dried microparticles were placed on double-sided adhesive carbon stickers (Provac AG, Balzers, Liechtenstein) and coated with 5 nm of platinum. The micrographs were taken on a LEO 1530 GEMINI scanning electron microscope (Zeiss, Cambridge, UK).

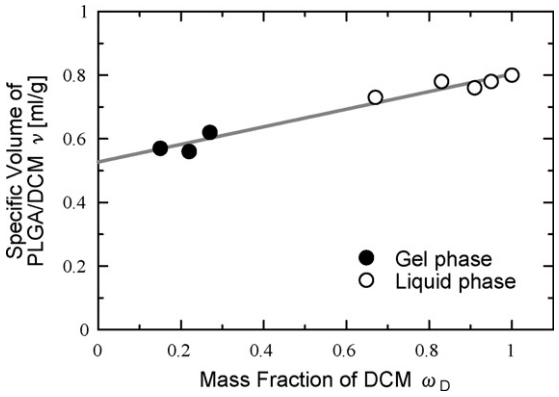

Fig. 3. Relationship between specific volume of PLGA/DCM solution and mass fraction of DCM.

4. Results

4.1. Duration of solvent extraction

A linear relationship was determined between the specific volume of PLGA/DCM solution, ν, and the mass fraction of DCM, ω_D, as expressed by: $\nu = 0.267w_d + 0.527$ [ml/g] (Fig. 3). In the mass fraction range of 0.3–0.6, the samples appeared inhomogeneous with a gel-like layer on the surface and liquid phase below; therefore, this range was excluded from the experimental analysis. The product of the specific volume times the mass fraction of DCM yields the concentration of DCM (ml/g) in the samples. Therefore, the plotting of the specific volume, ν, against the product of $\nu \cdot \omega_D$ yields the specific volume of the PLGA solution/film as a function of DCM concentration, which corresponds to the function, $\nu(c_{df})$, described in Section 2.2 and required to integrate Eq. (8).

Measured and calculated normalized amounts of residual DCM during solvent evaporation from pure DCM (gray undulated profile) and from PLGA/DCM solution/film (black undulated profile) are shown in Fig. 4. The calculated profiles (dotted lines) were obtained from Eqs. (4)–(8) by varying the diffusion coefficients from 1×10^{-8} to 1×10^{-5} cm^2/s. The measured evaporation profiles of pure DCM matched closely those calculated with diffusion coefficients in the range of 1×10^{-6} to 1×10^{-5} cm^2/s. On the other hand, the measured DCM evaporation from PLGA/DCM solution/film was substantially slower and matched the calculated profile with a diffusion coefficient of 2×10^{-7} cm^2/s.

Considering diffusion coefficients of 2×10^{-7} and 1×10^{-5} cm^2/s (Cussler, 1997) for DCM in PLGA and in pure solvent, respectively, the kinetics of DCM extraction from the center of a PLGA/DCM droplet of 2 μm in diameter was calculated following the model

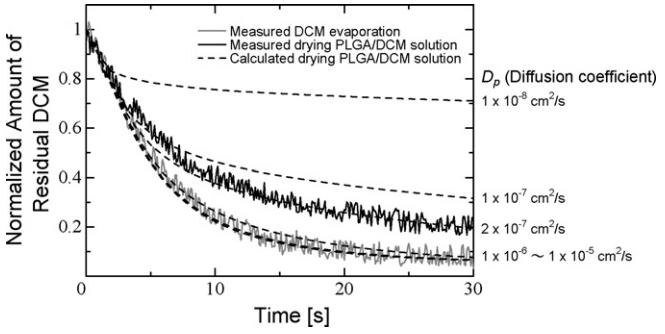

Fig. 4. Comparison between measured and predicted profiles of residual normalized amounts of DCM in PLGA/DCM. Experiments were performed with a 7.5% (w/w) solution of PLGA in DCM.

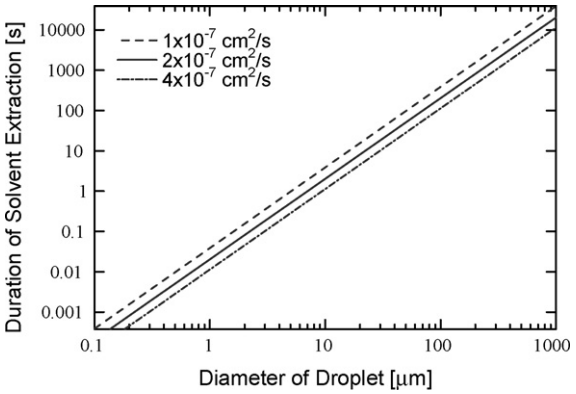

Fig. 5. Predicted relationship between the duration of solvent extraction and the diameter of micro- or nanoparticles using diffusion coefficients of 1×10^{-7}, 2×10^{-7}, 4×10^{-7} cm^2/s.

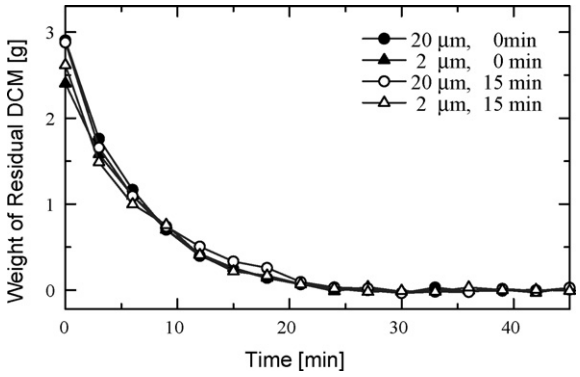

Fig. 7. Evaporation profiles of DCM from PLGA/DCM droplets dispersed in pure water; the droplet mode diameters used, d_{mod}, were 2 and 20 μm; before the solvent evaporation step, the solvent extraction time was either 0 or 15 min.

described in Section 2.1. The model predicts that 99.9% of solvent, relative to initial concentration, is extracted from the center of the droplet within approx. 0.1 s. The predicted solvent extraction time for smaller and larger PLGA/DCM droplets and for solvent diffusion coefficients of 1×10^{-7}, 2×10^{-7}, 4×10^{-7} cm^2/s is illustrated in Fig. 5. According to this model, solvent extraction is a very fast process, which does not take longer than a few minutes even for particles as large as 100 μm.

The microchannel-operated mixer used for the emulsification of the PLGA/DCM-phase (o-phase) in the w-phase (Fig. 1, Step 1) produced droplet sizes in the range of 0.5–100 μm, which was controlled by the flow rate of the fluids (Fig. 6(a)). With increasing flow rates (i.e., from 2/20 (o-phase/w-phase) ml/min to 10/100 ml/min) the droplet sizes became smaller and the size distributions narrower and monomodal. The plot of the mode diameter, d_{mod} (i.e., most frequent particle diameter) versus fluids flow rate illustrates that d_{mod} can readily be controlled between 2 and 20 μm and that d_{mod} is particularly sensitive to changes in flow rate between 20 and 50 ml/min (Fig. 6(b)). Considering now the droplet sizes produced (Fig. 6), the determined solvent extraction time for such droplets (Fig. 5), and the time for processing the fluids in the micromixer (15–75 s for 27.5 ml fluid at total flow rates of 110–22 ml/min), it can be concluded that in the present experiments virtually all DCM was extracted into the water phase during the processing in the micromixer. Therefore, the time needed for solvent removal in the preparation of PLGA microparticles by conventional solvent extraction/evaporation must primarily be governed by the solvent evaporation from the aqueous extraction phase.

4.2. Duration of solvent evaporation from the extraction phase and its importance for the morphology of dried polymer particles

The model and deduced data for the solvent evaporation from the extraction phase were validated through fabrication of batches of large (d_{mod} of 20 μm) and small microparticles (d_{mod} of 2 μm). As described above, the particle slurry was discharged from the micromixer into a cylindrical sealed vessel for solvent extraction during either 0 or 15 min (Fig. 1, Step 2), before being transferred into a large glass dish to monitor solvent evaporation during 45 min (Fig. 1, Step 3). This experiment aimed at elucidating whether a prolonged solvent extraction time of 15 min (Step 2) would alter the solvent evaporation kinetics, which would suggest differences in residual solvent in the PLGA/DCM droplets upon discharge from the micromixer. For example, if a substantial amount of solvent was still present in the PLGA/DCM particles at discharge from the micromixer, the evaporation rate of the subsequent Step 3 would be lower due to a lower solvent concentration in the extraction medium. The actual data demonstrate that no difference of solvent evaporation rate was noticed between the different particle sizes and extraction times (Fig. 7).

The knowledge of the solvent evaporation rate from the extraction phase (Fig. 7) should also give an indication about the time point when the particles can be separated from the slurry. From previous experiments it was known that a premature filtration of the slurry (e.g., after 10 or 20 min) through a membrane filter for particle collection yields, upon drying, a polymer film on the filter rather than a powdery product; this was ascribed to the residual solvent in the extraction phase exerting a plastizising effect on the surface of the microparticles during drying. According to the

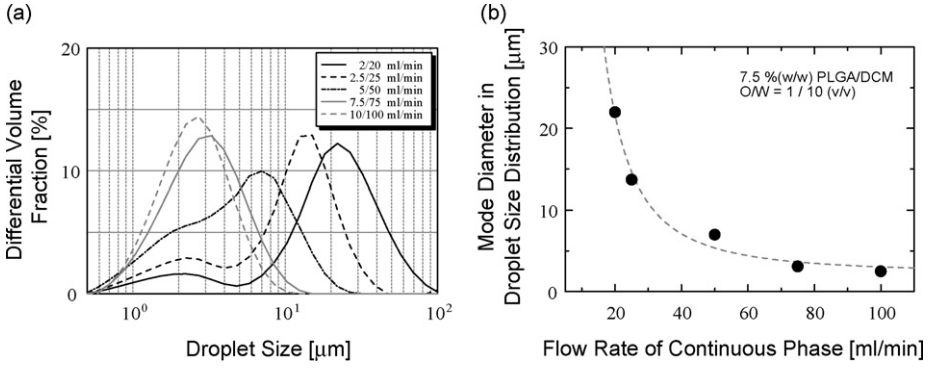

Fig. 6. Control of PLGA/DCM droplet size by the micro-channel-operated micromixer: (a) size distributions of PLGA/DCM droplets as a function of fluid feed-rate; (b) mode diameter (d_{mod}) as a function of flow rate of the continuous phase in the micromixer (o/w ratio was 1/10 (v/v)).

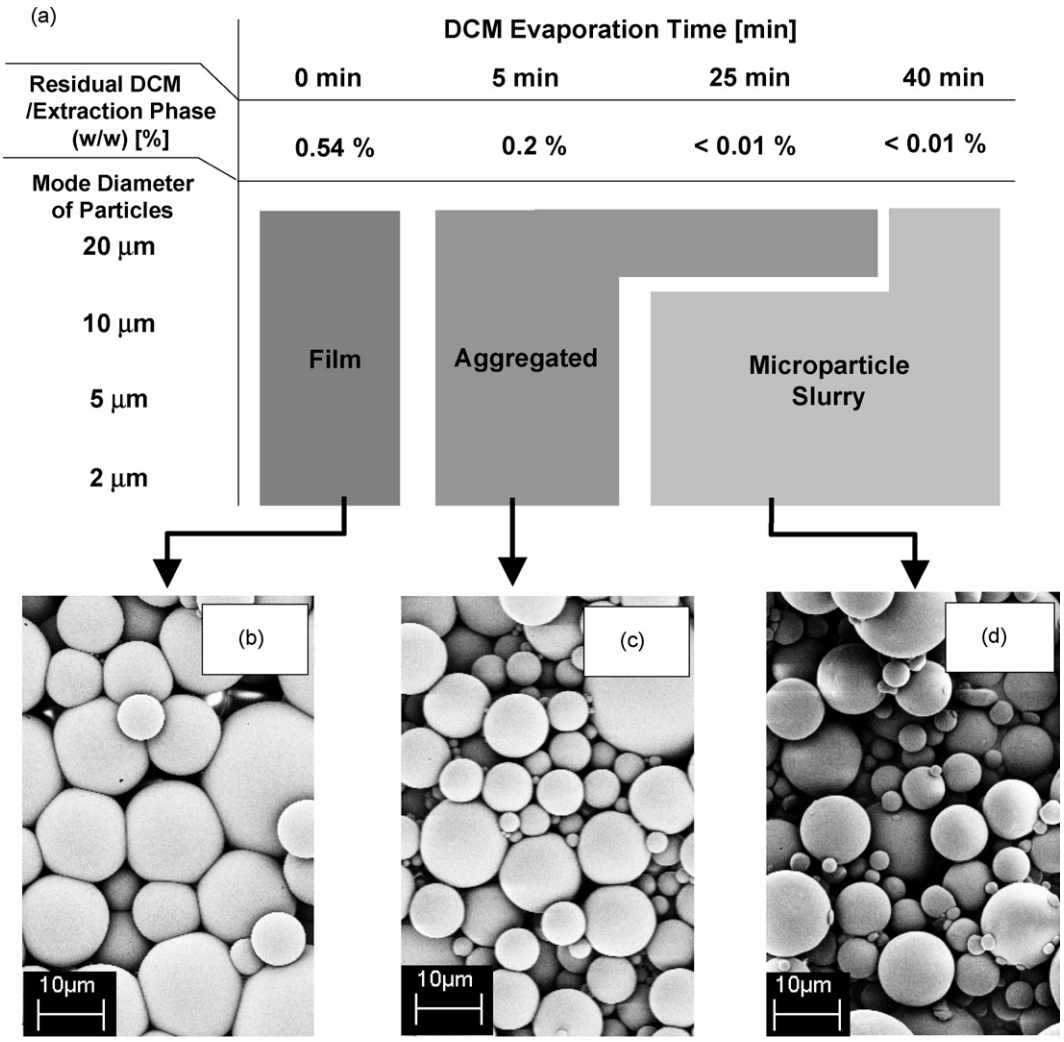

Fig. 8. Effects of evaporation time and residual DCM (extracted from PLGA/DCM droplets) in extraction phase on the morphology of the dried PLGA products; (a) macroscopic appearance of the PLGA products; (b–d) SEM micrographs of the dried products; (b) very strongly aggregated PLGA particles (macroscopic appearance of a "film"; (c) partially aggregated PLGA particles (macroscopic appearance of "aggregates"); (d) non-aggregated particles.

data of Fig. 7, DCM was evaporated to a large extent after 40 min under the actual experimental conditions. To examine the effect of residual DCM in the extraction phase on the morphology of dried PLGA particles with d_{mod} of 20, 10, 5 or 2 μm (Fig. 8), the PLGA particle slurry was filtered either before the solvent evaporation step (0 min) or after 5, 25 or 40 min during evaporation; the products were finally dried on the membrane filters. All products (with different d_{mod}) collected before solvent evaporation (0 min; DCM concentration in extraction phase: approx. 0.54%) formed a coherent film on the membrane filter, which could be readily peeled off in the wet state and became hard and brittle upon drying. The products collected after 5 min of solvent evaporation (DCM concentration in extraction phase: 0.2%) formed firm aggregates during drying, which required intense grinding for breaking them up into individual microparticles. Similar aggregates formed from large particles (d_{mod} of 20 μm) after solvent evaporation for 25 min (DCM concentration in extraction phase: <0.01%). This duration of solvent evaporation was, however, sufficient to obtain a fine powdery product of non-aggregated particles with the smaller-sized particle batches (d_{mod} of 10, 5 and 2 μm). The products collected after 40 min of solvent evaporation consisted, after drying, exclusively of non-aggreated microparticles, irrespective of particle size. Surprisingly, the SEM images of dried particles with a d_{mod} of 20 μm revealed particulate morphologies for all samples irrespective of their macroscopic appearance (film, aggregates, fine powder) (Fig. 8). The microscopic appearances only differed in the 3D arrangement and density of arrangement of the particles. With the film, the particulate arrangement was very dense and appeared flat, whereas the non-aggregated microparticles showed a loose and pronounced 3D arrangement. The aggregated state appeared microscopically intermediate between those of the film and the non-aggregated microparticles.

5. Discussion

The main objectives of the present study were the investigation of the kinetics of solvent extraction and evaporation for PLGA microparticle fabrication from an o/w-dispersion and the establishment of mathematical models for predicting the process kinetics. Experiments and mathematical models indicated unambiguously that, under the actual conditions, DCM extraction from PLGA/DCM droplets proceeds much faster than the DCM evaporation from the aqueous extraction phase. A striking visual confirmation of the fast DCM extraction was obtained by scanning electron microsopy of the dried product that was collected immediately after discharge

from the micromixer, i.e., only a few seconds after formation of the o/w-dispersion. Although this product formed macroscopically a film upon collection and drying on a membrane filter, individual and completely non-coalesced particulate morphologies were observed microscopically. This proves that most solvent had been removed from the particles at their discharge from the micromixer so that coalescence did not occur even under filtration pressure. The sticking together of the individual microparticles upon drying must be attributed to the residual solvent in the extraction phase that remained adsorbed on the particles before their final drying. Therefore, it is the solvent evaporation step in the described microparticle fabrication process that defines the overall processing time.

The high rate of DCM extraction into the aqueous phase was predicted by the mathematical model developed in this study. Solvent extraction under the actual experimental conditions was governed mainly by solvent diffusion in the polymer droplets. We estimated the DCM diffusibility in PLGA by a simple experimental method and derived a diffusion coefficient of 2×10^{-7} cm^2/s at room temperature, although the actual diffusibility in PLGA/DCM is not constant, but varies with PLGA concentration. In a previous study, DCM diffusion coefficient values in PLGA/DCM at room temperature were estimated theoretically to be in the order of 10^{-5} to 10^{-4} cm^2/s at low polymer concentration and approx. 10^{-9} cm^2/s at high concentration (Li et al., 1995a). Diffusion coefficients of DCM in PLGA have also been determined by inverse gas chromatography at 80–120 °C and found to be in the range of $(3.5–11) \times 10^{-7}$ cm^2/s (Eser and Tihminlioglu, 2006). The PLGA glass transition temperatures, as calculated from the Kelley–Bueche equation (Li et al., 1995a), are 49 °C for pure PLGA and 25 °C in the presence of 10% DCM. Therefore, at 80–120 °C the PLGA is in the rubbery state. Thus, the diffusion coefficient of DCM determined in our study is in the range of values reported in the literature and represents the diffusibility of DCM in PLGA in its rubbery state.

The validity of the predicted diffusion coefficient was also confirmed experimentally by the very fast formation of well-defined microparticles after mixing the o- and w-phases in the micromixer. For example, for particle sizes with $d_{mod} = 20$ μm, the diffusion-based model predicted a solvent extraction time of approx. 10 s. Experimentally, we showed that well-defined non-coalesced microparticles could be collected on a membrane filter right after the discharge of the o/w-dispersion from the micromixer, which represents a total processing time of 75 s for the batch size used (Fig. 8(b)). Thus, most of the solvent was extracted from the o-phase directly after the emulsification.

The present study stresses the importance of residual organic solvent concentration in the extraction phase for the morphology of the final product. Although there are reports on solvent diffusibility (Wang and Schwendeman, 1999; Li et al., 1995a) and on solvent residues in microparticles (Li et al., 1995a; Graham et al., 1999), we are not aware of studies considering the effect of solvent content in the extraction phase on the morphology of the final microparticulate product. Early methods to speed up the process of solvent evaporation from the aqueous extraction phase used either slightly elevated temperatures (Jeyanthi et al., 1996) or reduced pressure (Chung et al., 2002). The limited temperature increase accelerates the solvent evaporation only slightly, whereas the application of reduced pressure may cause substantial pore formation in the microparticles. Technically more viable ways of solvent evaporation or removal from the extraction phase would be needed for industrialization purposes.

From this study we derive that the knowledge and control of solvent diffusion in the polymer phase and solvent evaporation from a solvent extraction phase are critical and instrumental for the successful fabrication of microparticles. Knowledge of the critical parameters will also allow one to adapt and optimize the solvent extraction/evaporation process to any types of polymers, solvents and extraction phases. We expect that the developed tools and methods, involving experimental and theoretical techniques, will contribute to future optimization of process conditions and final products.

6. Conclusion

We derived a mathematical model for predicting the solvent extraction kinetics from a PLGA/DCM-in-water-dispersion. The solvent diffusion coefficient required for this model was determined by a simple experiment. From the model, the duration of solvent extraction was predicted for different PLGA/DCM droplet/particle sizes. The model was validated by the fabrication of PLGA microparticles with d_{mod} of 2- and 20-μm, for which the model predicted a solvent extraction time of approx. 0.1 and 10 s, respectively. In the microparticle fabrication method, conducted in a novel micromixer, the minimal processing time for the 240 mg particle batches was 15 and 75 s for the 2 and 20 μm particles, respectively. After these processing times, well defined and non-coalescent microparticles were obtained. The study further predicted and evidenced that the removal of most of the organic solvent from the extraction phase (below 0.2% (w/w) residual solvent in extraction phase) was necessary for obtaining non-aggregated particles after collection by filtration and drying. The time of solvent evaporation was much longer than the time for solvent extraction so that the former defined the total processing time required. Finally, the presented method and data should be a useful tool and guideline for the optimization and industrialization of solvent extraction/evaporation-based microparticle fabrication processes.

Acknowledgements

The authors gratefully acknowledge constructive comments and useful advises made by Prof. Hans Peter Merkle and Dr. Stefan Fischer (currently, F. Hoffmann-La Roche, Basel) from the Institute of Pharmaceutical Science, ETH Zurich.

References

Babin, V., Holyst, R., 2005. Evaporation of a sub-micrometer droplet. J. Phys. Chem. B 109, 11367–11372.
Berkland, C., Kim, K., Pack, D.W., 2001. Fabrication of PLG microspheres with precisely controlled and monodisperse size distributions. J. Control. Release 73, 59–74.
Birdi, K.S., Vu, D.T., Winter, A., 1989. A Study of the evaporation rates of small water drops placed on a solid surface. J. Phys. Chem. 93, 3702–3703.
Chen, J.-L., Yeh, M.-K., Chiang, C.-H., 2004. The mechanism of surface-indented protein-loaded PLGA microparticle formation: the effect of salt (NaCl) on the solidification process. J. Microencapsul. 21, 877–888.
Chung, T.W., Huang, Y.Y., Tsai, Y.L., Liu, Y.Z., 2002. Effects of solvent evaporation rate on the properties of protein-loaded PLLA and PDLLA microspheres fabricated by emulsion-solvent evaporation process. J. Microencapsul. 19, 463–471.
Cussler, E.L., 1997. Diffusion Mass Transfer in Fluid Systems, 2nd ed. Cambridge University Press, Cambridge, 127 pp.
Erbil, H.Y., Dogan, M., 2000. Determination of diffusion coefficient–vapor pressure product of some liquids from hanging drop evaporation. Langmuir 16, 9267–9273.
Eser, H., Tihminlioglu, F., 2006. Determination of thermodynamic and transport properties of solvents and non-solvents in poly(L-lactide-co-glycolide). J. Appl. Polym. Sci. 102, 2426–2432.
Fang, X., Li, B., Petersen, E., Ji, Y., Sokolov, J.C., Rafailovich, M.H., 2005. Factor controlling the drop evaporation constant. J. Phys. Chem. B 109, 20554–20557.
Flory, P.J., 1978. Principle of Polymer Chemistry, 10th ed. Cornel University Press, New York, pp. 495–511.
Freitas, S., Merkle, H.P., Gander, B., 2004. Ultrasonic atomization into reduced pressure atomosphere—envisaging aseptic spray-drying for microencapsulation. J. Control. Release 95, 185–195.
Freitas, S., Rudolf, B., Merkle, H.P., Gander, B., 2005. Flow-through ultrasonic emulsification combined with static micromixing for aseptic production of microspheres by solvent extraction. Eur. J. Pharm. Biopharm. 61, 181–187.
Graham, P.D., Brodbeck, K.J., McHugh, A.J., 1999. Phase inversion dynamics of PLGA solutions related to drug delivery. J. Control. Release 58, 233–245.

Graves, R.L., Makoid, M.C., Jonnalagadda, S., 2005. The effect of coencapsulation of bovine insulin with cyclodextrins in ethylcellulose microcapsules. J. Microencapsul. 22, 661–670.
Hopkins, R.J., Reid, J.P., 2005. Evaporation of ethanol/water droplets: examining the temporal evolution of droplet size, composition and temperature. J. Phys. Chem. A 109, 7923–7931.
Jeyanthi, R., Thanoo, B.C., Metha, R.C., DeLuca, P.P., 1996. Effect of solvent removal technique on the matrix characteristics of polylactide/glycolide microspheres for peptide delivery. J. Control. Release 38, 235–244.
Li, G., Butt, H.-J., Graf, K.-H., 2006. Microstructures by solvent drop evaporation on polymer surface. Langmuir 22, 11395–11399.
Li, W.-I., Anderson, K.W., DeLuca, P.P., 1995a. Kinetic and thermodynamic modeling of the formation of polymeric microspheres using solvent extraction/evaporation method. J. Control. Release 37, 187–198.
Li, W.-I., Anderson, K.W., Mehta, R.C., DeLuca, P.P., 1995b. Prediction of solvent removal profile and effect on properties for peptide-loaded PLGA microspheres prepared by solvent extraction/evaporation method. J. Control. Release 37, 199–214.
Maa, Y.-F., Hsu, C., 1996. Microencapsulation reactor scale-up by dimensional analysis. J. Microencapsul. 13, 53–66.
Price Jr., P.E., Cairncross, R.A., 1999. Optimization of single-zone drying of polymer solution coatings to avoid blister defects. Dry. Technol. 17, 1303–1311.
Rowan, S.M., Newton, M.I., McHale, G., 1995. Evaporation of microdroplets and the wetting of solid surface. J. Phys. Chem. 99, 13268–13271.
Wang, J., Schwendeman, S.P., 1999. Mechanisms of solvent evaporation encapsulation processes: prediction of solvent evaporation rate. J. Pharm. Sci. 88, 1090–1099.
Zhang, J.X., Zhu, K.J., 2004. An improvement of double emulsion technique for preparing bovine serum albumin-loaded PLGA microspheres. J. Microencapsul. 21, 775–785.